

*Full Length Research Paper*

# Geotechnical and geological studies of NWCT tunnel in Iran focusing on the stabilization analysis and design of support: A case study

Vahed Ghiasi<sup>1\*</sup>, Husaini Omar<sup>1</sup>, Jamal Rostami<sup>2</sup>, Zainuddin B. Md. Yusoff<sup>1</sup>, Samad Ghiasi<sup>3</sup>,  
Bujang .K. Huat<sup>1</sup> and Ratnasamy Muniandy<sup>1</sup>

<sup>1</sup>Department of Civil Engineering, Faculty of Engineering, University Putra Malaysia 43400, Serdang, Selangor, Malaysia.

<sup>2</sup>Department of Energy and Mineral Engineering, Penn State University, USA.

<sup>3</sup>Tehran Urban and Suburban Railway Company(TUSRC),Iran

Accepted 30 November, 2010

**In this paper, a detailed geomechanical investigation of rock masses of North Water Convey Tunnel (NWCT) and its stability analysis has been carried out. The NWCT is located in the north of Iran and is to be constructed in-order to convey water for agriculture purposes. The main instability in the tunnel is joints and faults. The rocks mass encountered in the tunnel route are made of argillaceous, sandstone and shale. The tunnel has been divided into two parts, lot1 and lot2 having a length of 14 km and 26 km respectively. It is proposed to be constructed by telescopic shield method using a tunnel boring machine (TBM). In this study, the most suitable methods are utilized for the stability analysis and design of support of the tunnel. For the empirical investigation, the rock mass were classified based on RMR, Q, RSR, GSI and Rmi systems. The geomechanical properties of the rock mass were determined from the laboratory and field investigations. The results obtained from the analysis show that the tunnel is highly unstable due to the presence of a fault and hence strong supports are need in these regions. The support system used is concrete lining, as the tunnel in used for water conveyance. The tunnel alignment in lot1 is divided into 12 lithology types as; LI-SH1, LI-SH2, LI-SH3, LI-SH4, LI1, LI2, LI3, LI4, LI5, SI, CZ and FZ regions. Similarly, the tunnel alignment in lot2 is divided into 21 lithology types as; SH-ML1, SH-ML2, SH-ML3, MLI-SH1, ML-SH2, ML-SH3, ML-SH4, ML-SH5, SH-LS1, SH-LS2, SH-LS3, SH-LS4, LI2, LI3, LI4, LI5, LI6, LI-MA, LI-SH, CZ, FZ regions. A stability analysis is a necessity as during the tunneling instabilities, such as the presence of a shear zones, may cause an obstruction and delaying of TBM progressing rate.**

**Key words:** Tunnel boring, stability analysis, rock mass classification system, empirical and numerical methods, support pressure.

## INTRODUCTION

The NWCT tunnel, located in north of Iran, provides a part of water requirement to the north Iran tropical plains (Figure 1). The inlet and outlet portals of the tunnel are 635 m and 625 m higher respectively than the free water level and the maximum overburden point of this tunnel is 800 m. This paper presents the geological study of the complete tunnel path, including lot1 and lot2. The total length of the tunnel is 40 km; 14 km in lot1 and 26 km in

lot2. The dip along the length of the tunnel is about 8/1000.

These experimental methods adopted in this study are based on the results of different thicknesses of the strata obtained by the boreholes used for the analyses of stability of the tunnel.

This study reflects the findings of the 40 km long tunnel area constructed by the TBM. The geometry of the tunnel shape is circular and the parameters of tunnel properties have been shown in Table 1. The geological study included the field and laboratories investigations and based on the results, the tunnel alignment of lot1 and lot

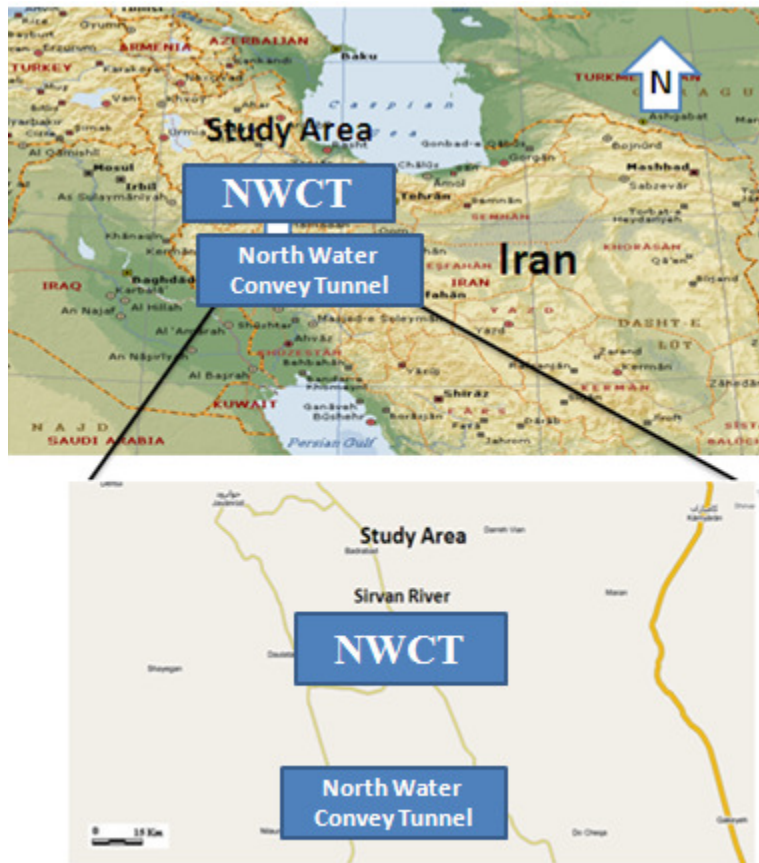


Figure 1. Location of studied area in Iran.

Table 1. General parameters of the tunnel path.

Parameters	Properties	
Length of tunnel path	Lot 1	14 km
	Lot 2	26 km
Inlet tunnel free water surface		625 m
Outlet tunnel free water surface		635 m
Radius of tunnel boring operation		2.3 m
Maximum overburden		800 m
Dip		8/1000

2 was divided into 12 and 21 lithology types respectively.

### Geological conditions

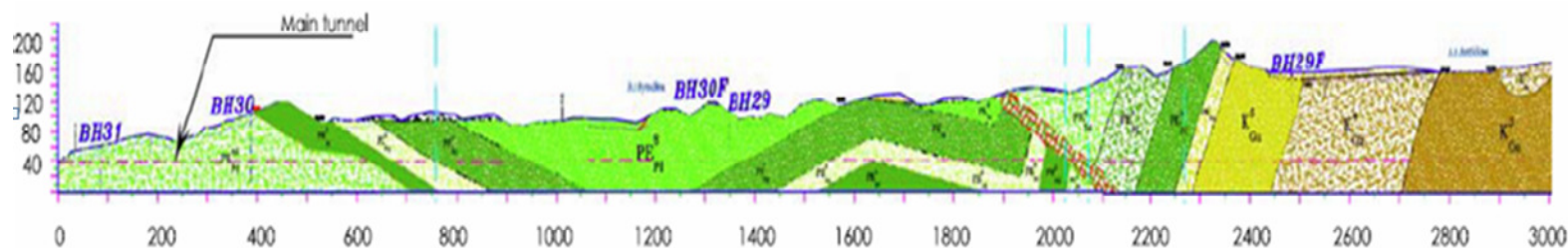
Based on the results of the samples and boreholes carried out, the transfer tunnel path passes through argillaceous sandstone and shale type of soil/rock as shown in (Figure 2).

Some stability problems were predicted at some locations along the alignment and hence a more detailed exploration was carried out. These locations are as

follows:

1. Tunnel entrance.
2. Distance from some parts of the tunnel alignment to ground level may be low because at these places, the rocks are weak.
3. Depth of weathered rocks is high.
4. Shear regions and comminuted, and
5. Aquifer horizons.

Based on the results of studies made in the engineering geological zone, along the total route of the tunnel, regardless of surface sediments or hypothesis, the lithology of the rock/soil has been identified to include debris such as argillaceous and shale, sandstone and shale. The investigation of the types of lithology in tunnel path of lot 1 and lot2 was carried out. According to the field and visual investigation, including geological and geotechnical investigation (borehole, core logging and laboratory testing), the rock/soil mass has been identified to consist of 12 lithography types in lot 1 and 21 lithography types in lot2. The types of lithology identified are shown in Tables 2 and 3. The boundaries of types of lithography are according to the stratigraphy and in many cases for the geomechanical features, the lithography



Geology	SH-ML1, SH-ML2	ML-SH1	ML-SH2	ML-SH3	ML-SH2	SH-ML3	ML-SH2	ML-SH1	ML-SH4	ML-SH5	SH-LS1	SH-LS2	SH-LS3
Lithology	Argillaceous and shale										Argillaceous and shale, sandstone and shale		
Structure	Layered, jointed, folded		Layered	Layered, jointed, folded	Layered				Fractured		Jointed, folded		Layered, folded
Average permeability (m/sec)	15e <sup>-8</sup>		2.5e <sup>-8</sup>						15e <sup>-8</sup>		1e <sup>-7</sup>		

Figure 2. Longitudinal geological profiles of the excavated sections of NWCT (lot2).

was the main factor in separation and classification.

The category classification of massif regional characteristics in geomechanical features is illustrated in Table 4.

As is evident from Table 2, the rock mass, along the tunnel path in lot1, varies from very weak, thinly bedded, crushed and unstable to moderately strong, thick bedding and stable. Similarly, the rock mass along the tunnel path in lot2 (Table 3) varies from very weak, thin bedding, crushed and unstable to weak to moderately strong, crushed, medium bedding and unstable.

Also, based on the geomechanical features, the rock mass in lot1 consists of poor and crushed to

very strong, massive with an average distance between discontinuities of significantly more than half a meter. Similarly, the geomechanical features in lot2 can be described as poor and crushed to semi-solid, medium to thick layers and the average distance between the discontinuities to be significantly less than half a meter.

A large number of tests were performed for geotechnical classification of the rock/soil mass. The characteristics included, rock strength, density, uniaxial tensile strength, shear strength parameters, Young's modulus and hardness to abrasion. The determination of the properties requires accurate sampling of all the samples of the rocks and perform laboratory tests on samples

of the above mentioned and identify the basic lithology along the tunnel path. The physical and mechanical properties of the rock units along tunnel alignment in lot1 and lot 2 were evaluated and are presented in Tables 5 and 6 respectively.

### Engineering classification of rock mass

A number of methods are available to classify a rock mass based on a variety of parameters (Cai et al., 2007). Apuani et al. (2005) have also tried to find the physical and mechanical properties of rock masses at Stromboli. A specific upscaling theory of rock mass parameters exhibiting spatial

**Table 2.** Lithology of rock mass along tunnel (lot1).

Geology	Stability state	
	Description	Type
LI-SH1	Weak to moderately strong, crushed, moderately bedding, unstable	B
LI-SH2	Moderately weak, thin bedding, crushed almost unstable	C
LI-SH3	Moderately weak, thin bedding, crushed almost unstable	C
LI-SH4	Weak to moderately strong, crushed, moderately bedding, unstable	B
LI1	Moderately strong, thick bedding, little crushing, stable	A
LI2	Moderately strong, thick bedding, little crushing, stable	A
LI3	Moderately strong, thick bedding, little crushing, stable	A
LI4	Moderately strong, thick bedding, little crushing, stable	A
LI5	Weak to moderately strong, crushed, bedding medium, unstable	B
SI	Moderately weak, thin bedding, crushed almost unstable	C
CZ	Very weak, thin bedding, crushed and unstable	D
FZ	Moderately weak, thin bedding, crushed almost unstable	C

**Table 3.** Property of rock mass in different units (lot 2).

Geology	Stability State	
	Description	Type
SH-ML1	Moderately weak, thin bedding, crushed almost unstable	C
SH-ML2	Very weak, thin bedding, crushed and unstable	D
SH-ML3	Very weak, thin bedding, crushed and unstable	D
MLI-SH1	Weak to moderately strong, crushed, bedding medium, unstable	B
ML-SH2	Moderately weak, thin bedding, crushed almost unstable	C
ML-SH3	Moderately weak, thin bedding, crushed almost unstable	C
ML-SH4	Moderately weak, thin bedding, crushed almost unstable	C
ML-SH5	Weak to moderately strong, crushed, bedding medium, unstable	B
SH-LS1	Very weak, thin bedding, crushed and unstable	D
SH-LS2	Moderately weak, thin bedding, crushed almost unstable	C
SH-LS3	Relatively weak, thin bedding, crushed almost unstable	C
SH-LS4	Very weak, thin bedding, crushed and unstable	D
LI2	Very weak, thin bedding, crushed and unstable	D
LI3	Weak to moderately strong, crushed, bedding medium, unstable	B
LI4	Moderately weak, thin bedding, crushed almost unstable	C
LI5	Weak to moderately strong, crushed, bedding medium, unstable	B
LI6	Weak to moderately strong, crushed, bedding medium, unstable	B
LI-MA	Moderately weak, thin bedding, crushed almost unstable	C
LI-SH	Moderately weak, thin bedding, crushed almost unstable	C
CZ	Very weak, thin bedding, crushed and unstable	D
FZ	Very weak, thin bedding, crushed and unstable	D

**Table 4.** Category classification of massif regional characteristics and geomechanical features.

Type	Geomechanical features
A	Very strong, massive, the average distance between discontinuities being significantly more than half a meter
B	Semi-solid to solid, medium to thick layers, the average distance between discontinuity being significantly less than half a meter
C	Semi-solid to weak, thin to medium layer, the average distance of discontinuity significantly less than 0.2 m
D	Poor, crushed

**Table 5.** Physical and geotechnical properties of the rock along tunnel alignment (lot 1).

Geology	Uniaxial compressive strength (MPa)	Tensile Strength (MPa)	Modulus of deformation (GPa)	Saturated density (g/cm <sup>3</sup> )	Porosity (%)	Weathering in surfaces
LI-SH1	5-25(20)* 100-150(125)**	1-2.5*, 10-15**	2-5*, 15-25**	2.5-2.7	5-15	Moderately weathered
LI-SH2	50-100(75)	5-10	5-25	2.35-2.85	5-10	Highly weathered
LI-SH3	5-25(20)* 50-100(75)**	2.5-10	2-6	2.3-2.7	1-5	Moderately weathered
LI-SH4	5-25(20)* 50-100(75)**	2.5-10	2-6*, 20-50**	2.4-2.65	2-6	Slightly weathered
LI1	5-25(20)* 50-100(75)**	1-2.5, 5-10	15-25	2.5-2.7	5-15	Slightly weathered
LI2	100-150(125)	2.5-10	4-8, 15-25	2.35-2.85	0.5-5.5	Moderately weathered
LO3	100-150(125)	5-15	5-15	2.65-2.85	0.5-2	Moderately weathered
LI4	100-150(125)	5-10	15-25	2.5-2.7	0.5-2	Slightly weathered
LI5	50-100(75)	5-15	5-10*, 40-70**	2.45-2.75	1-8	Slightly weathered
SI1	25-50(35)	0.5-1	2-5	2.6-2.7	1-2	Moderately weathered

\*Shale; \*\*lime

**Table 6.** Physical and geotechnical properties of the rock along tunnel alignment (lot 2).

Geology	Uniaxial compressive strength (MPa)	Tensile strength (MPa)	Modulus of deformation (GPa)	Dry density (g/cm <sup>3</sup> )	Porosity (%)	Weathering in surfaces
SH-ML1	25-50(35)	1-3	4-6	2.4-2.5	10-15	Moderately weathered
SH-ML2	25-50(35)	1-3	4-6	2.3-2.5	10-15	Highly weathered
SH-ML3	25-50(35)	1-3	5-6.5	2.3-2.5	5-15	Moderately weathered
ML-SH1	50-100(75)	1-3	4-6.5	2.5-2.6	2-5	Slightly weathered
ML-SH2	25-50(35)	1-3	4-6.5	2.2-2.5	5-10	Slightly weathered
ML-SH3	25-50(35)	2-4	5-6	2.05-2.5	5-15	Moderately weathered
ML-SH4	25-50(35)	2-4	4-6	2.2-2.5	5-10	Moderately weathered
ML-SH5	50-100(75)	5-10	5.5-7	2.3-2.6	3-5	Slightly weathered
SH-LS1	5-25(20)	1-3	4-6	2.4-2.5	3-15	Slightly weathered
SH-LS2	25-50(35)	2-4	5-6	2.3-2.6	3-10	Moderately weathered
SH-LS3	5-25(20)	1-3	4-6	2.3-2.5	5-15	Moderately weathered
SH-LS4	25-50(35)	1-2, 2-5	4-6, 2-4	2.3-2.6	5-10	Moderately weathered
LI2	100-150(125)	2.5-6	15-30	2.5-2.6	2-5	Slightly weathered
LI3	100-150(125)	5-10	15-30	2.5-2.6	2-5	Slightly weathered
LI4	50-100(75)	2.5-6	5-10	2.5-2.6	2-5	Slightly weathered
LI5	100-150(125)	2.5-6	5-10	1.9-2.7	5-15	Slightly weathered
LI6	100-150(125)	5-10	15-30	2.5-2.5	2-5	Slightly weathered
LI-MA	25-50(35)	1-3	2-5	2.2-2.6	2-5	Moderately weathered
LI-SH	5-50(35)	1-3	2-5	2.2-2.6	2-5	Moderately weathered
CZ	5-150	5-10	5-7	2.5-2.6	2-5	Highly weathered
FZ	5-150	1-3	4-6	2.3-2.5	5-15	Highly weathered

variability was presented by Exadaktylos and Stavropoulou (2008). In this study, the rock mass classification were performed according to Rock Mass Rating (RMR), RMR modified, Geological Strength Index

(GSI), Rock Structure Rating (RSR), Quality system (Q), and Rock Mass index (RMI) systems for the transfer tunnel and the properties of rock mass were determined by using these systems. In order to apply the rock mass

**Table 7.** Classification of rock mass along tunnel path based on suggested systems (lot1).

Geology	RQD (%)	RMR	Modified RMR	Q	GSI	RMi	RSR
LI-SH1	75-90	36-56	26-46	1.9-5	25-30,50-56	1.05-4.3	
LI-SH2	50-75	40-45	38-43	2-2.5	35-40	1.5-2.0	
LI-SH3	50-90	37-45	35-42	1.5-2.5	30-50	2.5-3	
LI-SH4	50-75	45-50	43-48	1-4.17	35-50	1.26-2.47	
LI1	50-75	34-47	32-45	1.27-2.75	25-50	0.9-2.6	
LI2	50-75	50-52	48-50	2-2.75	45-55	3-4	
LI3	50-75	50-52	48-50	2.5-3	45-50	3-3.5	
LI4	75-90	50-56	48-54	4-5	48-53	4-5	
LI5	75-85	45-53	43-51	1.35-2.2	45-50	2-2.5	
SI	25-50	30-36	25-31	0.5-1	30-40	0.5-1	
FZ	25-50	36-38	34-36	0.5-1	25-35	0.5-1	
CZ	0-50	25-38	23-36	0.3-0.5	18-35	0.5	

classification systems, the tunnel alignment were divided into nine different zones; each of which has its own independent engineering properties. The RMR system was initially developed by Bieniawski (1974) on the basis of his experiences in shallow tunnels and was modified further (Bieniawski, 1989). The studied parameters are rock quality designation (RQD), uniaxial compressive strength (UCS), discontinuity spacing, discontinuity condition, groundwater condition and discontinuity orientation. RQD has been used by Palmstrom (2005) for the measurements of and correlations between block size and rock quality designation.

The GSI is a new rock mass classification system that was developed by Hoek (1994) and Hoek et al. (1995). This classification system is based on the structure of the rock mass and does not suggest a direct correlation between rock mass quality and GSI. Therefore, it can be estimated based on the correlation between GSI and RMR values.

The Q-system was developed as a rock tunneling quality index by Norwegian Geotechnical Institute (NGI) (Barton et al., 1974) and the last improved version was released in 2004. The Q-value can be calculated as follows:

$$Q = \frac{RQD}{J_n} \times \frac{J_r}{J_a} \times \frac{J_w}{SRF} \quad (1)$$

This classification system includes six parameters of rock quality as following:

1. Rock quality designation (RQD)
2. The number of joint sets ( $J_n$ )
3. The joint surface roughness ( $J_r$ )
4. The degree of joint weathering and alteration ( $J_a$ )
5. Joint water reduction factor ( $J_w$ )
6. Stress reduction factor (SRF)

The three quotients in Equation (1) may be taken to represent the block size, the inter-block frictional shear strength and the active stress respectively.

Goel et al. (1995) suggested the parameter  $Q_n$ , for stress free form Q. In order to calculate  $Q_n$ , SRF is taken 1, which has been given in Equation (2):

$$Q_n = \left( \frac{RQD}{J_n} \times \frac{J_r}{J_a} \right) \times J_w \quad (2)$$

$$Q_c = Q \frac{\sigma_c}{100} \quad (3)$$

Where,  $Q_c$  is uniaxial compressive strength (MPa) of the intact rock mass. These classification systems are used to estimate the rock mass parameters along the tunnel alignment and the results have been presented in Tables 7 and 8 for lot1 and lot2 respectively.

### Determination of rock mass strength parameters

#### The generalized Hoek-Brown criterion

The generalized Hoek-Brown failure criterion for jointed rock masses is defined by:

$$\sigma_1' = \sigma_3' + \sigma_{ci} \left( m_b \frac{\sigma_3'}{\sigma_{ci}} + s \right)^a \quad (4)$$

Where,  $\sigma_1'$  and  $\sigma_3'$  are the maximum and minimum effective principal stresses at failure,  $m_b$  is the value of the Hoek-Brown constant m for the rock mass,  $S$  and  $a$  are constants which depend upon the rock mass

**Table 8.** Classification of rock mass along tunnel path based on suggested systems (lot2).

Geology	RQD (%)	RMR	Modified RMR	Q	GSI	RMi	RSR
SH-ML1	50-75	45-50	35-40	3-3.5	35-45	0.5-1.5	37
SH-ML2	50-75	40-45	30-35	1.5-2	25-35	0.5-1	28
SH-ML3	50-75	40-50	30-40	2-2.5	40-45	1-2	38
ML-SH1	75-90	60-65	50-55	6-6.5	40-55	8-12	54
ML-SH2	50-75	45-50	35-40	2.5-3	45-50	2.5-3.5	46
ML-SH3	50-75	45-50	35-40	2-2.5	35-45	2-2.5	40
ML-SH4	50-75	50-55	40-45	3.5-4	40-45	4.5-5.5	45
ML-SH5	75-90	60-65	50-55	5-6	40-55	8-12	52
SH-LS1	50-75	40-45	30-35	2-3	35-40	0.5-1.5	37
SH-LS2	50-75	45-50	35-45	4-4.5	40-45	2.5-3	39
SH-LS3	50-75	45-50	35-40	2.5-3	35-40	1-2	37
SH-LS4	75-90	40-50	35-45	1.5-2	40-45	1-2	40
LI2	75-90	55-65	45-55	4-5	55-60	6-7	54
LI3	75-90	55-65	45-55	5.5-6	55-60	7-8	54
LI4	75-90	50-60	40-50	2-2.5	40-45	3-4	54
LI5	75-90	50-60	45-55	5-5.5	50-55	7-7.5	61
LI6	90-100	65-70	60-65	10-12	60-65	8-10	65
LI-MA	50-75	40-45	30-40	1.5-2	35-40	1-2	43
LI-SH	50-75	40-45	35-40	2-3	35-45	1.5-2.5	47
FZ	25-50	30-40	20-30	1-2	25-30	0.5-1	32
CZ	5-25	20-30	18-25	0.5-1	15-25	0025-0.75	26

**Table 9.** The result of engineering rock classification for different unites (lot 2).

Unite	RQD (%)	RMR	Modified RMR	Q	GSI	RMi	RSR
SH-ML1	50-75	45-50	35-40	3-3.5	35-45	0.5-1.5	37
SH-ML2	50-75	40-45	30-35	1.5-2	25-35	0.5-1	28
SH-ML3	50-75	40-50	30-40	2-2.5	40-45	1-2	38
ML-SH1	75-90	60-65	50-55	6-6.5	40-55	8-12	54
ML-SH2	50-75	45-50	35-40	2.5-3	45-50	2.5-3.5	46
ML-SH3	50-75	45-50	35-40	2-2.5	35-45	2-2.5	40
ML-SH4	50-75	50-55	40-45	3.5-4	40-45	4.5-5.5	45
ML-SH5	75-90	60-65	50-55	5-6	40-55	8-12	52
SH-LS1	50-75	40-45	30-35	2-3	35-40	0.5-1.5	37
SH-LS2	50-75	45-50	35-45	4-4.5	40-45	2.5-3	39
SH-LS3	50-75	45-50	35-40	2.5-3	35-40	1-2	37
SH-LS4	75-90	40-50	35-45	1.5-2	40-45	1-2	40
LI2	75-90	55-65	45-55	4-5	55-60	6-7	54
LI3	75-90	55-65	45-55	5.5-6	55-60	7-8	54
LI4	75-90	50-60	40-50	2-2.5	40-45	3-4	54
LI5	75-90	50-60	45-55	5-5.5	50-55	7-7.5	61
LI6	90-100	65-70	60-65	10-12	60-65	8-10	65
LI-MA	50-75	40-45	30-40	1.5-2	35-40	1-2	43
LI-SH	50-75	40-45	35-40	2-3	35-45	1.5-2.5	47
FZ	25-50	30-40	20-30	1-2	25-30	0.5-1	32
CZ	5-25	20-30	18-25	0.5-1	15-25	0025-0.75	26

characteristics, and  $\sigma_{ci}$  is the uniaxial compressive strength of the intact rock pieces.

In order to use the Hoek-Brown criterion for estimating the strength and deformability of jointed rock masses, three properties of the rock mass have to be estimated.

These are:

1. Uniaxial compressive strength  $\sigma_{ci}$  of the intact rock mass,
2. Value of the Hoek-Brown constant  $m_b$  for these intact rock mass, and
3. Value of the geological strength index (GSI) of the rock mass.

The relationship between the principal stresses at failure for a given rock is defined by two constants, the uniaxial compressive strength  $\sigma_{ci}$  and a constant  $m_i$ . Wherever possible, the values of these constants should be determined by statistical analysis of the results of a set of triaxial tests on carefully prepared core samples.

One should note that the range of minor principal stress ( $\sigma_3'$ ) values over which these tests are carried out is critical in determining reliable values for the two constants. In deriving the original values of  $\sigma_{ci}$  and  $m_i$ , Hoek and Brown (1980a) used a range of  $0 < \sigma_3' < 0.5\sigma_{ci}$  and, in order to be consistent, it is essential that the same range be used in any laboratory triaxial tests on intact rock specimens. At least five well spaced data points should be included in the analysis.

The influence of blast damage on the near surface rock mass properties has been taken into account in the 2000 version of the Hoek-Brown criterion (Hoek et al., 2000) as follows:

$$m_b = m_i \exp\left(\frac{GSI - 100}{28 - 14D}\right) \quad (5)$$

$$S = \exp\left(\frac{GSI - 100}{9 - 3D}\right) \quad (6)$$

$$a = \frac{1}{2} + \frac{1}{6} \left( e^{-GSI/15} - e^{-20/3} \right) \quad (7)$$

Where,  $D$  is a factor which depends upon the degree of disturbance due to blast damage and stress relaxation. It varies from 0 for undisturbed in situ rock masses to 1 for very disturbed rock masses. For this project, according to the method of tunneling  $D$  is taken as 0.

### Rock mass parameters

The most important rock mass parameters for safe tunnel design are the deformation modulus ( $E_{mass}$ ), uniaxial

compressive strength of rock mass ( $\sigma_{mass}$ ) and Hoek-Brown constants. The physical and mechanical properties of the various rock units along tunnel alignment such as porosity, unit weight, uniaxial compressive strength, tensile strength and shear strength parameters ( $c$  and  $\phi$ ) were determined by performing laboratory tests. The results have been presented in Tables 10, 11, 12, 13, 14, 15, 16, 17, 18, 19, 20, 21, and 22.

As evident from Tables 12, 14, 16 and 18, the friction angle of the joints along the tunnel path varies from a low of  $7.6^\circ$  to as high as  $42^\circ$ . Similarly, the cohesion (Tables 13, 15, 17 and 19) of joints along the tunnel length varied from 0.04 MPa to 2.04 MPa.

The cohesion, internal friction angle, tensile strength, comparative strength, total comparative strength and deformation modulus were determined, as said earlier, and shown in Tables 19, 20, 21 and 22. It is seen from these tables that the cohesion of the rock mass varies from a low of 0.39 MPa to as high as 3.5 MPa. Similarly, the angle of internal friction of the rock mass varies from  $23^\circ$ - $53^\circ$ .

### Strength of rock mass

It is important to understand the rock mass behavior and failure mechanism for safe design of underground spaces and tunnels (Stavropoulou et al., 2007). Although, the estimation of rock mass is carried out for the safe design and stabilization of excavated spaces, it will be difficult because of the presence of the planes of weakness cause anisotropy in rock properties (Basarir, 2008; Deb and Das, 2010; Tzamos and Sofianos, 2007). However, the main aim is to provide the estimate of the strength and deformation properties of the rock mass and to provide an initial estimate of the support requirements for safe design.

Bhasin and Grimstad (1996) have suggested to use eq. (8) for hard rocks,  $\sigma_{ci} > 100$  (MPa) and  $Q > 10$ , where  $\gamma$  is the unit weight of rock mass in  $t/m^3$ .

$$\sigma_{mass} = \left(\frac{\sigma_{ci}}{100}\right) 7\gamma Q^{\frac{1}{3}} \quad (\text{MPa}) \quad (8)$$

Singh et al. (1997) have modified the equation for  $Q < 10$ :

$$\sigma_{mass} = 7\gamma Q^{\frac{1}{3}} \quad (\text{MPa}) \quad (9)$$

Trueman (1998) calculated the strength of rock mass by using RMR, as below:

$$\sigma_{mass} = 0.5e^{0.06RMR} \quad (\text{MPa}) \quad (10)$$

Barton (2000) expressed rock mass strength ( $\sigma_{mass}$ )



**Table 10.** Strength parameters of fractures (As per Barton formula).

Barton shear failure criterion					
Joint set 2 Gate 1					
Input parameters					
Basic friction angle ( $\phi$ )				25	
Joint roughness coefficient (JRC)				6	
Joint compressive strength (JCS)				150	
Minimum normal stress				2	
Output parameters					
Normal stress ( $\sigma_n$ ) (MPa)	Shear strength ( $\tau$ ) (MPa)	$d_r$ $d_{\sigma n}$ (DTDS)	Friction angle ( $\phi$ ) (degree)	Cohesive strength ( $c$ ) (MPa)	
0	0	-----	-----	-----	
0.25	0.222	0.808	39.0	0.020	
0.5	0.418	0.758	37.2	0.039	
0.75	0.603	0.729	36.1	0.056	
1	0.783	0.710	35.4	0.073	
2	1.466	0.663	33.6	0.140	
3	2.116	0.637	32.5	0.204	
4	2.743	0.619	31.8	0.267	
5	3.355	0.443	23.9	1.140	
6	3.954	0.401	21.9	1.548	
7	4.543	0.379	20.7	1.894	
8	5.124	0.337	18.6	2.425	
9	5.696	0.312	17.3	2.887	
10	6.262	0.290	16.2	3.363	
11	6.822	0.270	15.1	3.852	
12	7.377	0.252	14.2	4.351	
13	7.927	0.236	13.3	4.861	
14	8.472	0.221	12.5	5.380	
15	9.013	0.207	11.7	5.908	
16	9.550	0.194	11.0	6.443	
17	10.083	0.182	10.3	6.987	

**Table 11.** Internal friction angle ( $\phi$ ) (degree) of rock joints along tunnel length (0-3 km) (lot 2).

Geology	SH-ML1	SH-ML2	SH-ML3	ML-SH1	ML-SH2	ML-SH3	ML-SH4	ML-SH5	SH-LS1	SH-LS2	SH-LS3	CZ1	CZ2	FZ1
Joint 1	31	28.8	28.9	42	40.5	38	34.7	34.7	29.1	21.37	29.1	28	22	21
Joint 2	23.5	27.9	25.8	33.5	26.9	32	27.06	29.1	28.2	31	29.9	22	22	22
Joint 3	25.6	27.3	29.9	38	31	38	38.9	29.1	29.4	32	26.5	24	21	21
Joint 4	-	33.1	29.9	38	-	-	36.9	35.9	-	29.7	-	-	-	-
Bedding	35.3	35.3	28.8	38.9	36.6	38.9	35.9	37.6	27.6	29.7	28.9	24	23	21

using the normalization of Q-values, as below, where  $\gamma$  is the unit weight of rock mass ( $t/m^3$ ).

$$\sigma_{mass} = 5\gamma \left( Q \frac{\sigma_c}{100} \right)^{\frac{1}{3}} \text{ (MPa)} \quad (11)$$

The calculated  $\sigma_{mass}$  values have been given in Table 23.

The  $\sigma_{mass}$  obtained by Bhasin and Grimstad (1996) method is 496 MPa. It could be determined for only one segment of the tunnel path. It was observed that the values of  $\sigma_{mass}$  vary from 20.24-52.74 MPa, based on the

**Table 12.** Cohesion *c* (MPa) of rock joints along tunnel length (0-3 km) (lot 2).

Geology	SH-ML1	SH-ML2	SH-ML3	ML-SH1	ML-SH2	ML-SH3	ML-SH4	ML-SH5	SH-LS1	SH-LS2	SH-LS3	CZ1	CZ2	FZ1
Joint 1	0.077	0.026	0.148	0.158	0.151	0.094	0.255	0.255	0.243	0.053	0.243	0	0.1	0.1
Joint 2	0.014	0.038	0.097	0.034	0.019	0.083	0.088	0.092	0.182	0.155	0.112	0	0	0
Joint 3	0.029	0.05	0.112	0.094	0.081	0.094	0.189	0.092	0.13	0.118	0.074	0	0	0
Joint 4	-	0.041	0.112	0.094	-	-	0.135	0.176	-	0.226	-	-	-	-
Bedding	0.057	0.057	0.148	0.072	0.089	0.072	0.176	0.245	0.216	0.226	0.148	0	0	0.1

**Table 13.** Internal friction angle ( $\phi$ ) (degree) of rock joints along tunnel length (3-10 km) (lot 2)

Geology	SH-LS4	LI2	SH-LS3	SH-LS2	SH-LS1	ML-SH5	CZ	FZ
Joint 1	31	28.8	28.9	42	40.5	38	34.7	34.7
Joint 2	23.5	27.9	25.8	33.5	26.9	32	27.06	29.1
Joint 3	25.6	27.3	29.9	38	31	38	38.9	29.1
Joint 4	-	33.1	29.9	38	-	-	36.9	35.9
Bedding	35.3	35.3	28.8	38.9	36.6	38.9	35.9	37.6

**Table 14.** Cohesion *c* (MPa) of rock joints along tunnel length (3-10 km) (lot 2).

Geology	SH-LS4	LI2	SH-LS3	SH-LS2	SH-LS1	ML-SH5	CZ	FZ
Joint 1	0.19	0.04	0.11	0.23	0.18	0.2	0.07	0.07
Joint 2	0.08	0.04	0.11	0.2	0.06	0.05	0.03	0.08
Joint 3	0.05	0.12	0.13	0.19	0.8	0.11	0.04	0.11
Joint 4	-	0.23	-	0.26	-	0.17	0.02	0.09
Bedding	0.26	0.32	0.43	0.5	0.4	0.6	0.11	0.06

**Table 15.** Internal friction angle ( $\phi$ ) (degree) of rock joints along tunnel length (10-17 km) (lot 2).

Geology	SH-LS1	SH-LS2	SH-LS3	SH-LS4	LI2	ML-SH5	CZ
Joint 1	33	28	26.7	29	33	31.0	28
Joint 2	34	27.8	20.6	29	34	31	28.4
Joint 3	26	22.6	25.8	18	37	22.5	28.3
Joint 4	35	22.6	25.8	28.9	37	-	28.4
Bedding	35	28	28.9	25	25	25	7.6

**Table 16.** Cohesion *c* (MPa) of rock joints along tunnel length (10-17 km) (lot 2).

Geology	SH-LS1	SH-LS2	SH-LS3	SH-LS4	LI2	ML-SH5	CZ
Joint 1	0.25	0.103	0.99	0.105	0.17	0.11	0.03
Joint 2	0.15	0.152	0.65	0.105	0.11	0.11	0.02
Joint 3	0.97	0.67	0.15	1.04	0.18	0.99	0.03
Joint 4	0.17	0.67	0.15	0.155	0.18	-	0.02
Bedding	0.17	0.29	0.22	0.76	1.6	1.04	2.04

relationship suggested by Singh et al. (1977). It varies from 6.40-28.70 MPa as per Trueman (1998) relationship; and from 9.72-30.54 MPa as per Barton (2000) relationship. The  $\sigma_{mass}$  obtained using Trueman (1998) relationship is quite on the lower side.

**Deformation modulus of rock mass ( $E_{mass}$ )**

For determining the deformation modulus of rock masses along the tunnel alignment, different equations proposed by different researchers have been used as follow:

**Table 17.** Internal friction angle ( $\varphi$ ) (degree) of rock joints along tunnel length (17-26 km) (lot 2).

Geology	L1-SH	LI6	LI5	LI4	LI3	LI-MA	CZ	FZ
Joint 1	26.5	32	28	30	35	25.0	18	27
Joint 2	28.3	24	36	27	19	23	25	27.4
Joint 3	26	36	37	32	21.6	28	28	29
Joint 4	-	-	-	-	-	31	28	28
Bedding	26	27	33	15	20	25	20	27

**Table 18.** Cohesion  $c$  (MPa) of rock joints along tunnel length (17-26 km) (lot 2).

Geology	L1-SH	LI6	LI5	LI4	LI3	LI-MA	CZ	FZ
Joint 1	0.5	0.22	0.7	0.09	0.26	0.5	0.9	0.14
Joint 2	0.2	1.5	0.2	0.4	2.4	0.9	0.08	0.06
Joint 3	0.8	0.18	0.1	0.16	2.5	0.15	0.04	0.04
Joint 4	-	-	-	-	-	0.16	0.07	0.08
Bedding	0.6	1.1	0.32	3.5	3	0.8	0.8	0.16

**Table 19.** Strength of rock mass in tunnel (0-3 km) (lot 2).

Geology	Cohesion (MPa)	Internal friction angle (degree)	Tensile strength (MPa)	Comparative strength (MPa)	Total comparative strength (MPa)	Deformation modulus (MPa)
SH-ML1	0.156	36.43	-0.017	0.34	1.69	1414
SH-ML2	0.134	34.43	-0.012	0.24	1.46	1060
CZ1	0.219	35.04	-0.007	0.24	1.91	1056
ML-SH1	3.486	30.51	-0.160	4.22	12.20	8367
SH-ML3	0.166	38.31	-0.007	0.24	1.91	1060
ML-SH2	0.248	42.15	-0.039	0.83	2.93	2812
ML-SH3	0.243	40.77	-0.045	0.83	2.72	2812
CZ2	0.334	38.96	-0.037	0.84	3.64	2495
ML-SH4	0.350	35.11	-0.025	0.60	3.19	7746
ML-SH5	0.642	41.77	-0.070	1.81	5.23	2495
SH-LS1	0.242	29.97	-0.015	0.30	1.80	1186
SH-LS2	0.355	36.33	-0.032	0.72	3.12	2310
SH-LS3	0.278	31.86	-0.021	0.43	2.11	1581
FZ	0.242	29.97	-0.015	0.30	1.82	1186

Bieniawski (1978) has defined  $E_{mass}$  as below:

$$E_{mass} = 2RMR - 100 \text{ (GPa)} \quad RMR > 5 \quad (12)$$

Serafim and Pereira (1983) have proposed the Equation (14) for  $RMR < 50$ :

$$E_{mass} = 10^{\left(\frac{RMR-10}{40}\right)} \text{ (GPa)} \quad RMR < 50 \quad (13)$$

For  $Q > 1$  and generally for hard rocks, Grimstad and Barton (1993) have proposed the Equation (15):

$$E_{mass} = 25 \log Q \text{ (GPa)} \quad (14)$$

Mitri (1994) has defined the Equation (15) for determining  $E_{mass}$  based on  $E_i$ , as below:

$$E_{mass} = E_i \left[ 0.5 \left( 1 - \left\{ \cos \pi \frac{RMR}{100} \right\} \right) \right] \text{ (GPa)} \quad (15)$$

Singh et al. (1997) has proposed an equation for

**Table 20.** Strength of rock mass in tunnel (3-10 km) (lot 2).

Geology	Cohesion (MPa)	Internal friction angle (degree)	Tensile strength (MPa)	Comparative strength (MPa)	Total comparative strength (MPa)	Deformation modulus (MPa)
SH-LS1	0.47	29	-0.02	0.52	2.70	1732
SH-LS2	0.98	40	-0.08	2.02	7.80	5302
SH-LS3	0.64	33	-0.04	0.99	3.75	3080
SH-LS4	0.54	38	-0.06	1.34	4.20	4107
ML-SH5	0.77	42	-0.05	1.80	9.32	3652
LI2	1.18	49	-0.25	6.03	14.6	11548
CZ3	0.44	38	-0.02	0.60	6.10	1540
CZ4	0.45	33	-0.02	0.55	5.01	1372
FZ2	0.40	28	-0.01	0.35	2.37	1298
CZ5	0.39	26	-0.01	0.23	2.16	974

**Table 21.** Strength of rock mass in tunnel (10-17.5 km) (lot 2).

Geology	Cohesion (MPa)	Internal friction angle (degree)	Tensile strength (MPa)	Comparative strength (MPa)	Total comparative strength (MPa)	Deformation modulus (MPa)
SH-LS1	0.44	23	-0.015	0.299	1.824	1185
SH-LS2	0.99	37	-0.099	2.24	7.01	5302
SH-LS3	0.41	24	-0.015	0.299	1.824	1185
SH-LS4	0.73	41	-0.054	1.65	6.98	3976
ML-SH5	1.3	45	-0.158	4.48	15.6	1499
LI2	2.14	51	-0.50	12.05	29.21	13335
CZ3	0.4-0.7	26-40	-0.017- -0.036	0.25-1.2	2.5-12	1120-1778

**Table 22.** Strength of rock mass in tunnel (17.5-26 km) (lot 2).

Geology	Cohesion (MPa)	Internal friction angle (degree)	Tensile strength (MPa)	Comparative strength (MPa)	Total comparative strength (MPa)	Deformation modulus (MPa)
LI3	3.1-3.5	42-44	-0.42 - -0.61	10-13	24-27	1330-1770
LI4	1.6-1.7	36-37	-0.08 - -0.12	2.5-3.4	10.5-11.5	480-650
LI5	1.7-2.06	47-49	-0.29 - -0.42	7.5-10	22-24	100-130
LI6	1.7-2.1	52-53	-0.42 - -0.61	10-13	24-27	1330-1770
LI-MA	0.52-0.58	36-38	-0.05 - -0.07	0.95-1.3	4.5-5.0	250-350
LI-SH	1.05-1.15	33-35	-0.04 - -0.06	1.3-1.8	5.5-6.25	350-470
CZ	0.91-0.97	28-29	-0.015 - -0.018	0.5-0.59	5.6-6.1	130-150
FZ	0.64-0.75	39-42	-0.03 - -0.04	0.99-1.5	10.12	170-230

determining  $E_{mass}$  by using  $E_i$  and Hoek-Brown constants:

$$E_{mass} = E_i (S_m)^{1/1.4} \text{ (GPa)} \tag{16}$$

$$S_m = \frac{7\gamma Q^{\frac{1}{3}}}{\sigma_{ci}} \tag{17}$$

For weak rocks,  $\sigma_{ci} < 100$  MPa, Hoek and Brown (1998) have found a correlation between  $E_{mass}$  and GSI:

$$E_{mass} = \sqrt{\frac{\sigma_{ci}}{100}} \times 10^{\left(\frac{GSI-10}{40}\right)} \text{ (GPa)} \tag{18}$$

Read et al. (1999) have proposed the Equation (19) for calculating  $E_{mass}$  based on RMR value of rock mass.

$$E_{mass} = 0.1 \left( \frac{RMR}{10} \right)^3 \text{ (GPa)} \tag{19}$$

**Table 23.** Strength values ( $\sigma_{mass}$ ) obtained from different equations (lot 2).

Equation No.	8	9	10	11
SH-ML1	-----	25.40	8.64	12.80
SH-ML2	-----	20.24	6.40	10.20
SH-ML3	-----	52.74	8.64	11.08
ML-SH1	-----	71.56	21.26	21.33
ML-SH2	-----	22.56	6.40	11.61
ML-SH3	-----	20.41	6.4	10.27
ML-SH4	-----	25.56	11.67	12.86
ML-SH5	-----	30.27	21.26	19.25
SH-LS1	-----	23.27	6.40	9.72
SH-LS2	-----	27.80	8.64	13.98
SH-LS3	-----	23.54	8.64	9.83
SH-LS4	-----	20.69	7.4	10.40
LI2	-----	29.47	18.30	22.67
LI3	-----	32.00	18.30	24.61
LI4	-----	23.39	13.56	15.20
LI5	-----	28.00	13.56	21.53
LI6	49.6	-----	28.70	30.54
LI-MA	-----	20.25	6.40	9.98
LI-SH	-----	22.80	6.40	11.24

Barton (2002) expressed  $E_{mass}$  based on  $Q_c$ , as follows:

$$E_{mass} = 10Q_c^{\frac{1}{3}} \text{ (GPa)} \quad (20)$$

The calculated  $E_{mass}$  values have been given in Table 24.

The  $E_{mass}$  was calculated using various relationships as mentioned above and it was observed that it varies from a low of 0.24 GPa to a high of 35.0 GPa.

### In-situ stresses

The main origins of in-situ stresses are geological conditions and geological history of the area. The magnitude of in-situ stresses in rock mass can change from zero to high amounts, as much as rock strength. Based on the information that is obtained from measuring in-situ stresses in different places, the magnitude of horizontal stress is usually more than the vertical stress at shallow depths (less than 500 m); whereas, they tend to a hydrostatic state at a depth of about 1000 m below the surface. In this study, for a better understanding,  $\sigma_h$  is assumed to be equal to  $\sigma_v$  as suggested by Hoek (2003). The stresses at NWCT site have mainly arisen from tectonic forces and overburden pressures. For the determination of the stresses, no field or laboratory tests have been carried out. However, they were calculated as:

$$\sigma_v = \gamma Z \quad (21)$$

Where:  $\sigma_v$  = vertical stress ( $t/m^2$ ),  $\gamma$  = unit weight of rock mass average ( $2.62 t/m^3$ ), and  $Z$  = tunnel depth below surface in m.

### Evaluation of squeezing conditions

The squeezing of rock is a process of large deformation which occurs around the tunnel due to stress concentration and material properties and it is a major factor for predicting rock behavior in underground excavations. This phenomenon usually occurs in weak rocks under the influence of high pressures. As a consequence of squeezing, large ground deformation occurs around the tunnels and underground openings in poor rocks. Large deformations, low shear strength and high in-situ stresses are the most effective factors on the stability and convergence of tunnel walls and face. The magnitude of tunnel convergence, rate of deformation and extent of the yielding zone around the tunnel depend on rock mass properties and critical zone around the tunnel. Generally, rock type, rock mass strength, ground water flow, pore pressure, state of stress and support techniques are the most important effective factors on the squeezing behavior (Juneja et al., 2010; Kim et al., 2006; Farrokh et al., 2006; Panthi and Nilsen, 2006; Barla et al., 2010). Singh et al. (1992), based on 39 case histories, by collecting data on rock mass quality ( $Q$ ), and overburden ( $H$ ), defined an equation for predicting squeezing conditions:

$$H = 350Q^{\frac{1}{3}} \quad (22)$$

Where:  $H$  = overburden (m), and  $Q$  = rock mass quality.

For squeezing condition:

$$H \gg 350Q^{1/3}$$

Goel et al. (1995) have proposed a simple empirical approach which is based on the rock mass number ( $Q_n$ ), as follows:

$$H = (27 \times Q_n^{0.33}) B^{-0.1} \quad (23)$$

Where:

$H$  = overburden (m),  $B$  = tunnel span or diameter (m), and  $Q_n$  = rock mass number.

If the right side of the equation is equal or bigger than the left side, squeezing conditions will occur. Jethwa et al. (1984) defined Equation (24) for determining the degree of squeezing on the basis of the rock mass uniaxial compressive strength and the tunnel depth below the

**Table 24.** Calculated  $E_{mass}$  values from empirical methods for different rock mass (lot 2).

Equation	12	13	14	15	16	17	18	19	20
SH-ML1	---	8.60	12.80			0.73	1.4	10.72	14.82
SH-ML2	---	6.50	6.08			0.58	1.05	7.68	12.06
SH-ML3	---	7.50	8.81			0.63	1.50	9.12	13.11
ML-SH1	25	---	19.90			0.44	2.55	24.41	18.42
ML-SH2	---	8.66	11.00			0.66	1.74	10.72	14.01
ML-SH3	---	8.66	8.81			0.58	1.40	10.72	13.11
ML-SH4	5	---	14.35			0.73	1.50	14.47	15.53
ML-SH5	25	---	18.51			0.40	2.55	24.41	17.65
SH-LS1	---	6.50	9.95			1.64	0.99	7.68	13.57
SH-LS2	---	8.60	15.71			0.79	1.51	10.72	16.20
SH-LS3	---	8.60	11.00			1.18	0.99	10.72	14.01
SH-LS4	---	7.50	6.1			0.6	1.51	9.12	12.06
LI2	20	---	16.33			0.24	---	21.60	16.51
LI3	20	---	19.00			0.26	---	21.60	17.92
LI4	10	---	8.81			0.32	2.21	16.64	13.11
LI5	10	---	18.00			0.26	---	16.64	17.38
LI6	35	---	26.01			0.32	---	310.75	22.24
LI-MA	---	6.50	6.10			0.53	1.31	7.68	12.06
LI-SH	---	6.50	9.95			0.65	1.41	7.68	13.57

**Table 25.** Classification of squeezing behavior according to different approaches (lot2).

Equation	22
SH-ML1	518.07
SH-ML2	422.1
SH-ML3	458.85
ML-SH1	644.7
ML-SH2	490.35
ML-SH3	458.85
ML-SH4	543.55
ML-SH5	617.75
SH-LS1	474.95
SH-LS2	567
SH-LS3	490.35
SH-LS4	422.1
LI2	577.85
LI3	627.2
LI4	458.85
LI5	608.3
LI6	778.4
LI-MA	422.1
LI-SH	474.95

surface as:

$$N_c = \frac{\sigma_{cm}}{\gamma \times H} \tag{24}$$

The classification of squeezing behaviors, according to different approaches, has been given in Table 25.

As is evident from Table 25, the squeezing potential of rock mass in lot2 is very high and it varies from a low of 422.1 to a high of 778.4. These values are quite significant and it must be provided with suitable support lining.

**Support pressures**

Rock mass classification systems form the backbone of the empirical methods and were applied for the estimation of the support pressure and the design of tunnel support. In this study, for the estimation of support pressure ( $P_i$ ), Q and RMR classification systems have been used.

Unal (1983) has presented Eq. (25) which can be used to calculate the tunnel support pressure based on RMR:

$$P_i = (100 - RMR) \gamma \times \frac{B}{100} \tag{25}$$

Where:  $P_i$  = Support pressure (kg/m<sup>2</sup>),  $B$  = Tunnel width (m), and  $\gamma$  = Unit weight (t/m<sup>3</sup>)

Goel and Jethwa (1995), based on rock mass rating (RMR), have defined eq. (26) for predicting squeezing conditions in tunnels:

$$P = \frac{7.5B^{0.1} \times H^{0.5} - RMR}{20RMR} \tag{26}$$

**Table 26.** Support pressure using empirical equations for different zones (lot 2).

Equation	25
SH-ML1	5.92
SH-ML2	6.35
SH-ML3	6.07
ML-SH1	4.4
ML-SH2	3.51
ML-SH3	5.38
ML-SH4	5.13
ML-SH5	4.23
SH-LS1	6.48
SH-LS2	5.92
SH-LS3	5.92
SH-LS4	6.2
LI2	4.7
LI3	4.7
LI4	5.3
LI5	4.76
LI6	3.81
LI-MA	6.35
LI-SH	6.35

Where,  $P$  is support pressure (MPa),  $B$  is tunnel width (m) and  $H$  is tunnel depth below the surface (m).

The amount of support pressure has been calculated for all zones of the tunnel path. Also, the summary of offered relationships by some researchers for calculating support pressure has been presented in Table 26.

As seen from the Table 26, the support pressure varies from a low of 3.81 MPa to a high of 6.48 MPa. These pressures are quite significant and warrant suitable lining in the tunnel. There are a large number of various relationships for measuring the support pressure in tunnels and a few widely used relationships are shown in Table 27.

### Tunnel support assessment

The design of support for tunnels in weak rocks is an interactive method. There are different approaches for evaluating tunnel support system and the interaction between the surrounding rock mass and supporting system. In this study for the safe tunnel design, a combination of empirical methods was adopted.

### METHODS

In this study, the support systems were assessed based on RMR and Q classification systems. The suggested support systems, based on RMR system with stand up times for each geotechnical zone, have been presented in Table 28 and Figure 3, without

installation of the support systems, the maximum and minimum stand up times for zones.

Barton et al. (1974), relating the Q-index with the stability and support requirements of underground excavations, have defined an additional parameter which is called the equivalent dimension  $D_e$  of excavation. This dimension is obtained by dividing the span, diameter or wall height of excavation by a quantity called the Excavation Support Ratio, ESR. Hence:

$$D_e = \frac{\text{Excavation span, diameter or height (m)}}{\text{Excavation Support Ratio (ESR)}} \quad (27)$$

The value of ESR is the so-called excavation support ratio. It ranges between 0.5 and 5 and has been presented in a tabular form in a number of research papers for various types of excavations. For the diversion tunnel, the excavation support ratio, ESR is defined as 1.6. Hence, for an excavation span of 5 m, the equivalent dimension,  $D_e$ , is 3.13. Barton et al. (1974)'s equivalent dimension,  $D_e$ , plotted against the value of Q, is used to define a number of support categories in a chart published in the original paper. This chart has recently been updated by Grimstad and Barton (1993) to reflect the increasing use of steel fibres, reinforced shotcrete in underground excavation support. The estimated support categories for each geotechnical zone along the diversion tunnel have been shown in Figure 4. Also, the recommended types of support have been presented in Table 9.

### RESULTS

This study is a contribution to the investigations and support design of a tunnel project in Iran in difficult geological condition using a combination of empirical methods. NWCT is a project with complicated geological conditions and this paper discusses it as a case study.

A geological study, included the field and laboratories investigations, was carried out and based on the results, the tunnel alignment of lot1 and lot 2 was divided into 12 and 21 lithology types respectively. Some stability problems were predicted at some locations along the alignment and hence a more detailed exploration was carried out.

Based on the results of studies made in the engineering geological zone, along the total route of the tunnel, regardless of surface sediments or hypothesis, the lithology of the rock/soil was identified to include argillaceous and shale, sandstone and shale. According to the field and visual investigation, including geological and geotechnical investigation (borehole, core logging and laboratory testing), the rock/soil mass has been identified to consist of 12 lithography types in lot 1 and 21 lithography types in lot2.

The boundary of types of lithography are according to the stratigraphy and in many cases for the geomechanical features, the lithography was the main factor in separation and classification.

The rock mass, along the tunnel path in lot1, varies from very weak, thinly bedded, crushed and unstable to moderately strong, thick bedding and stable. Similarly, the rock mass along the tunnel path in lot2 (Table 3) varies from very weak, thin bedding, crushed and

**Table 27.** Different relationships suggested by some researchers for measuring support pressure.

	References	Equation
Rock mass parameters ( $\sigma_{mass}$ )	Bhasin and Grimstad (1996)	$\sigma_{mass} = \left(\frac{\sigma_{ci}}{100}\right) 7\gamma Q^{\frac{1}{3}}$
	Singh et al. (1997)	$\sigma_{mass} = 7\gamma Q^{\frac{1}{3}}$
	Trueman (1998)	$\sigma_{mass} = 0.5e^{0.06RMR}$
	Barton (2000)	$\sigma_{mass} = 5\gamma \left(Q \frac{\sigma_c}{100}\right)^{\frac{1}{3}}$
	Bieniawski (1978)	$E_{mass} = 2RMR - 100$
	Serafim and Pereira (1983)	$E_{mass} = 10^{\left(\frac{RMR-10}{40}\right)}$
	Grimstad and Barton (1993)	$E_{mass} = 25 \log Q$
Deformation modulus of rock mass ( $E_{mass}$ )	Mitri (1994)	$E_{mass} = E_i \left[ 0.5 \left( 1 - \left\{ \cos \pi \frac{RMR}{100} \right\} \right) \right]$
	Singh et al. (1997)	$E_{mass} = E_i (S_m)^{1/1.4}$
	Hoek and Brown (1998)	$E_{mass} = \sqrt{\frac{\sigma_{ci}}{100}} \times 10^{\left(\frac{GSI-10}{40}\right)}$
	Read et al. (1999)	$E_{mass} = 0.1 \left(\frac{RMR}{10}\right)^3$
	Barton (2002)	$E_{mass} = 10Q^{\frac{1}{3}}$
Constant of rock mass (m-s)	Hoek et al. (1995)	$m_b = m_i \exp\left(\frac{GSI-100}{28-14D}\right)$ $s = \exp\left(\frac{GSI-100}{9-3D}\right)$

**Table 28.** Suggested support systems, assessed based on rock mass rating system (RMR) with stand up times for each geotechnical zone.

RMR	Anchoring $\Phi$ 20 mm	Shotcrete	Ribs	Zone
81-100	-	-	-	-
61-80	Locally bolts in crown, 3 m long, spaced 2.5 m, with occasional wire mesh	50 mm in crown where required		ML-SH1, ML-SH5, LI6
41-60	Systematic bolts 4 m long, spaced 1.5-2 m in crown and walls with wire mesh in crown	50-100 mm in crown, 30 mm in sides		SH-ML1, SH-LS1, SH-ML2, SH-LS2, SH-ML3, SH-LS3, ML-SH2, SH-LS4, ML-SH3, LI2, LI3, ML-SH4, LI4, LI5, LI-MA, LI-SH
21-40	Systematic bolts 4-5 m long, spaced 1-1.5 m in crown and walls with wire mesh	100-150 mm in crown, 100 mm in sides	Light ribs spaced 1.5 m where required	
<20	Systematic bolts 5-6 m long, spaced 1-1.5 m in crown and walls with wire mesh. Bolt invert	150-200 mm in crown, 150 mm in sides and 50 mm in face	Medium to heavy ribs spaced 0.75 m with steel lagging and forepoling if required. Close invert	

unstable to weak to moderately strong, crushed, medium bedding and unstable.

Based on the geomechanical features, the rock mass in lot1 were observed to consist of poor and crushed to very strong, massive with an average distance between discontinuities of significantly more than half a meter. Similarly, the geomechanical features in lot2 were described as poor and crushed to semi-solid, medium to thick layers and the average distance between the

discontinuities to be significantly less than half a meter. A large number of tests were performed for geotechnical classification of the rock/soil mass. The characteristics included, rock strength, density, uniaxial tensile strength, shear strength parameters, Young's modulus and hardness to abrasion. The physical and mechanical properties of the rock units along tunnel alignment in lot1 and lot 2 were evaluated.

In this study, the rock mass classification were



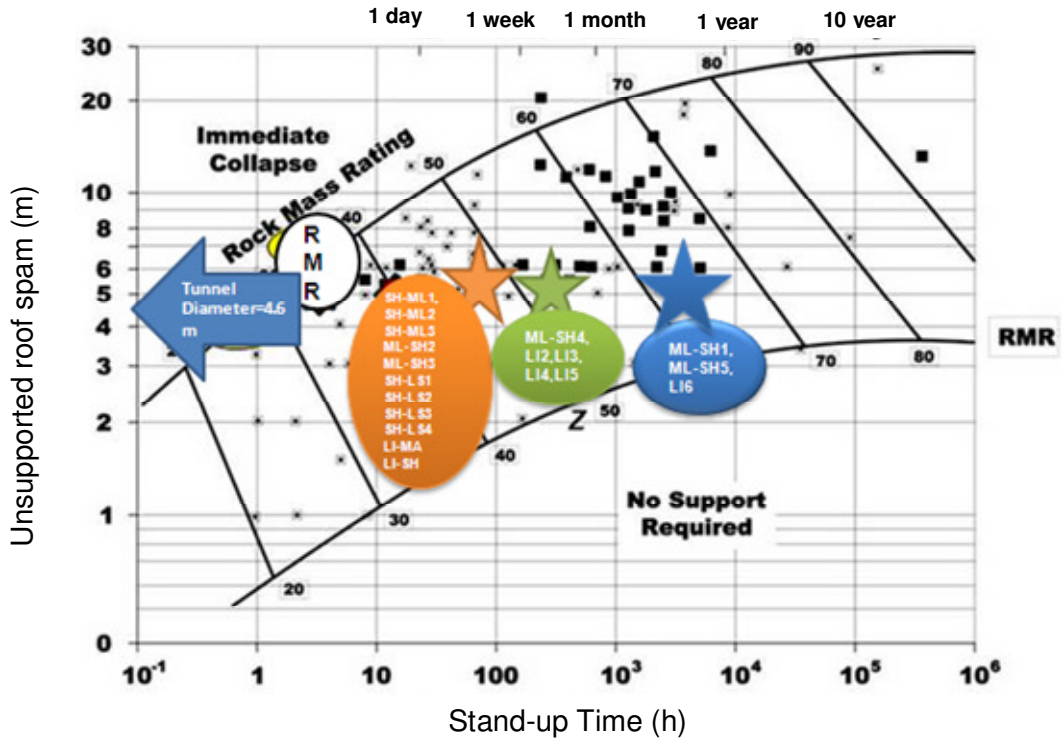


Figure 3. Relationship between Stand-up time, span and RMR classification (after Bieniawski, 1989).

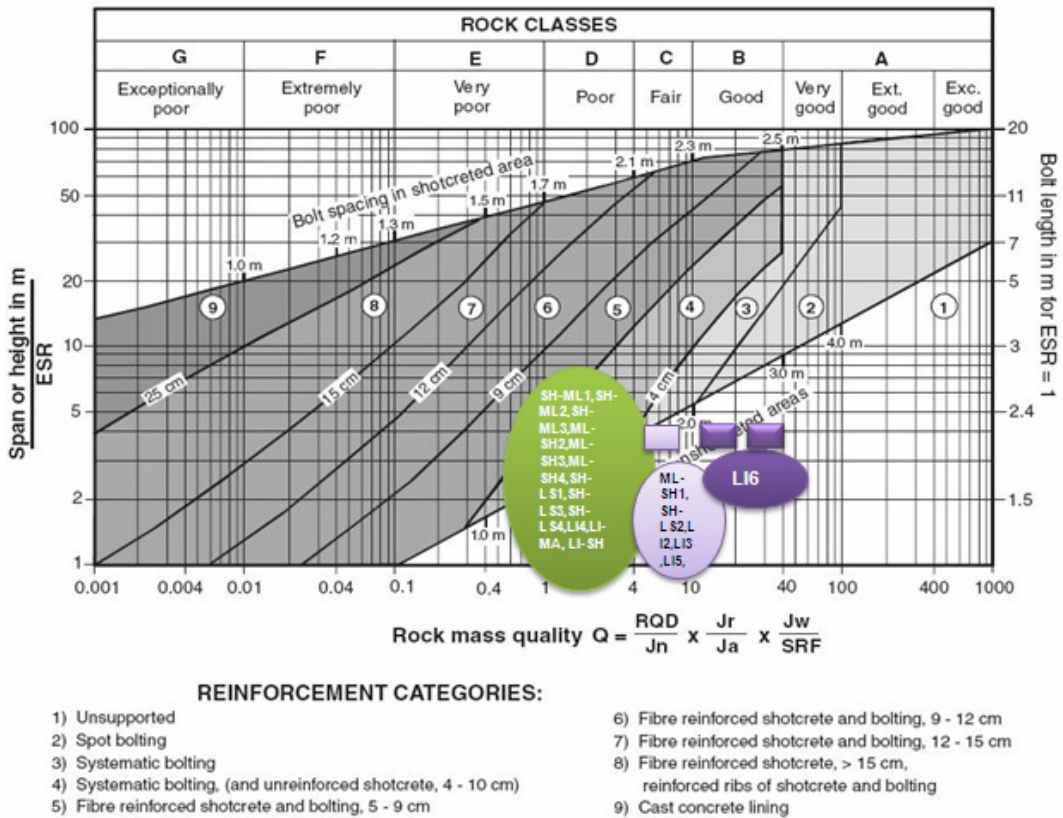


Figure 4. Estimated support categories based on the tunneling quality index Q (after, Palmstrom and Broch, 2006).

performed according to Rock Mass Rating (RMR), RMR modified, Geological Strength Index (GSI), Rock Structure Rating (RSR), Quality system (Q), and Rock Mass index (RMI) systems for the transfer tunnel and the properties of rock mass were determined by using these systems.

The most important rock mass parameters for safe tunnel design are the deformation modulus ( $E_{mass}$ ), uniaxial compressive strength of rock mass ( $\sigma_{cmass}$ ) and Hoek-Brown constants. The physical and mechanical properties of the various rock units along tunnel alignment such as porosity, unit weight, uniaxial compressive strength, tensile strength and shear strength parameters ( $c$  and  $\phi$ ) were determined by performing laboratory tests. The friction angle ( $\phi$ ) of the joints along the tunnel path varies from a low of  $7.6^\circ$  to as high as  $42^\circ$ . Similarly, the cohesion ( $c$ ) of joints along the tunnel length varied from 0.04 MPa to 2.04 MPa.

The cohesion, internal friction angle, tensile strength, comparative strength, total comparative strength and deformation modulus were determined. It was observed that the cohesion of the rock mass varies from a low of 0.39 MPa to as high as 3.5 MPa. Similarly, the angle of internal friction of the rock mass varies from  $23^\circ$ – $53^\circ$ .

It was observed that the values of  $\sigma_{cmass}$  vary from 20.24–52.74 MPa, based on the relationship suggested by Singh et al. (1977). It varies from 6.40–28.70 MPa as per Trueman (1998) relationship; and from 9.72–30.54 MPa as per Barton (2000) relationship. The  $\sigma_{cmass}$  obtained using Trueman (1998) relationship was quite on the lower side. Similarly, the deformation modulus ( $E_{mass}$ ) was calculated using various relationships as mentioned above and it was observed that it varies from a low of 0.24 GPa to a high of 35.0 GPa.

The squeezing of rock is a process of large deformation which occurs around the tunnel due to stress concentration and material properties and it is a major factor for predicting rock behavior in underground excavations. This phenomenon usually occurs in weak rocks under the influence of high pressures. The squeezing potential of rock mass in lot2 was observed to be very high and it varied from a low of 422.1 to a high of 778.4. These values were quite significant and it must be provided with suitable support lining.

Rock mass classification systems form the backbone of the empirical methods and were applied for the estimation of the support pressure and the design of tunnel support. The support pressure varied from a low of 3.81 MPa to a high of 6.48 MPa. These pressures were quite significant and warrant suitable lining in the tunnel.

There are different approaches for evaluating tunnel support system and the interaction between the surrounding rock mass and supporting system. The value of ESR is the so-called excavation support ratio. It ranged between 0.5 and 5 and has been presented in a tabular form in a number of research papers for various types of excavations. For the diversion tunnel, the excavation

support ratio, ESR is defined as 1.6. Hence, for an excavation span of 5 m, the equivalent dimension,  $D_e$ , is 3.13. Barton et al. (1974)'s equivalent dimension,  $D_e$ , plotted against the value of  $Q$ , was used to define a number of support categories in a chart published in the original paper. The estimated support categories for each geotechnical zone along the diversion tunnel have been shown, and also, the recommended types of support have been presented.

## Conclusions

A comprehensive engineering geological assessment of rock masses has been carried out at the site of NWCT in north of Iran. The geotechnical properties of these rocks have been carefully assessed based on the laboratory and field investigations for diversion tunnel support design. The classification results of the rock masses of tunnel alignment based on RMR, Q, GSI, RQD, RMI, modified RMR and RSR classification systems, shows that the rock mass available in lot1 is of 12 lithology types namely, LI-SH1, LI-SH2, LI-SH3, LI-SH4, LI1, LI2, LI3, LI4, LI5, SI, CZ and FZ. Similarly, there are 21 lithology types namely, SH-ML1, SH-ML2, SH-ML3, MLI-SH1, ML-SH2, ML-SH3, ML-SH4, ML-SH5, SH-LS1, SH-LS2, SH-LS3, SH-LS4, LI2, LI3, LI4, LI5, LI6, LI-MA, LI-SH, CZ, FZ along the tunnel alignment in lot2. These regions are classified as very poor and fair rocks argillaceous and shale, sandstone and shale. Based on the results, the tunnel alignment was divided into 12 and 21 (lot1 and lot 2) geotechnical zones and the tunnel support designs were accomplished by empirical method. The results obtained from different methods are in agreement with each other and for the safe tunnel support design, and using a combination of them is recommended.

## ACKNOWLEDGMENTS

The authors would like to thank all the persons, who have helped in some way or other, in preparing this case study. We would like to thank in particular M/s Sahel Consultants for their cooperation in providing the data and extending their help whenever required.

## REFERENCES

- Apuani T, Corazzato C, Cancelli A, Tibaldi A (2005). Physical and mechanical properties of rock masses at Stromboli: A dataset for volcano instability evaluation. Bull. Eng. Geol. Environ., 64(4): 419-431.
- Barla G, Debernardi D, Sterpi D (2010). Viscoplastic models for the analysis of tunnel reinforcement in squeezing rock conditions. Proc. Numerical Methods in Geotechnical Engineering (NUMGE), NTNU, Trondheim (Norway), June 2010.
- Barton NR, Lien R, Lunde J (1974). Engineering classification of rock masses for the design of tunnel support. Int. J. Rock Mech., 4: 189-239.

- Barton NR, Lien R, Lunde J (1974). Engineering classification of rock masses for the design of tunnel support. *Int. J. Rock Mech.*, 4: 189-239.
- Barton N (2000). *TBM Tunnelling in Jointed and Faulted Rock*. Rotterdam, Balkema, p. 169.
- Barton N (2002). Some new Q-value correlations to assist in site characterization and tunnel design. *Int. J. Rock Mech. Min. Sci.*, 39(1): 185-216.
- Basarir H (2008). Analysis of rock-support interaction using numerical and multiple regression modeling. *Can. Geotech. J.*, 45(1): 1-13.
- Bhasin R, Grimstad E (1996). The use of stress–strength relationships in the assessment of tunnel stability. *Tunneling Undergr. Space Technol.*, 11(1): 93-98.
- Bieniawski ZT (1974). Geomechanics classification of rock masses and its application in tunneling. *Proceedings of the Third International Congress on Rock Mechanics*. Int. Soc. Rock Mech. Denver, 11A: 27-32.
- Bieniawski ZT (1978). Determining rock mass deformability: experience from case histories. *Int. J. Rock Mech. Min. Sci. Geomech. Abstr.*, 15: 237–247.
- Bieniawski ZT. (1989). *Engineering Rock Mass Classifications*. Wiley, New York. p. 251.
- Cai M, Kaiser P, Tasaka Y, Minami M (2007). Determination of residual strength parameters of jointed rock masses using the GSI system. *Int. J. Rock Mech. Min. Sci.*, 44(2): 247-265.
- Carranza-Torres C, Fairhurst C (2000). Application of the convergence–confinement method of tunnel design to rock masses that satisfy the Hoek–Brown failure criterion. *Tunneling Undergr. Space Technol.*, 15(2): 187-213.
- Deb D, Das KC (2010). Extended Finite Element Method for the Analysis of Discontinuities in Rock Masses. *Geotech. Geol. Eng.*, 28(5), DOI 10.1007/s10706-010-9323-7.
- Exadaktylos G, Stavropoulou M (2008). A specific upscaling theory of rock mass parameters exhibiting spatial variability: Analytical relations and computational scheme. *Int. J. Rock Mech. Min. Sci.*, 45(7): 1102-1125.
- Farrokhi E, Mortazavi A, Shamsi G (2006). Evaluation of ground convergence and squeezing potential in the TBM driven Ghomroud tunnel project. *Tunneling Undergr. Space Technol.*, 21(5): 504-510.
- Goel RK, Jethwa JL, Paithakan AG (1995). Tunneling through the young Himalayas—A case history of the Maneri-Uttarkashi power tunnel. *Eng. Geol.*, 39: 31-44.
- Grimstad E, Barton N (1993). Updating the Q-system for NMT. *Proc. Int. Symp. on Sprayed Concrete*, Fagernes, Norway, Norwegian Concrete Association, Oslo, pp.20.
- Hoek E. 1994. Strength of rock and rock masses. *ISRM News J.*, 2(2): 4-16.
- Hoek E (2003). Numerical modelling for shallow tunnels in weak rocks. Unpublished notes. <http://www.rocscience.com>.
- Hoek E., Kaiser P.K., Bawden WF (1995). *Support of Underground Excavations in Hard Rock*. Balkema, Rotterdam, p. 215.
- Hoek E, Brown ET (1998). Practical estimates of rock mass strength. *Int. J. Rock Mech. Min. Sci.*, 34(8): 1165-1186.
- Jethwa JL, Singh B, Singh B (1984). Estimation of ultimate rock pressure for tunnel linings under squeezing rock conditions – a new approach. *Design and Performance of Underground Excavations*, ISRM Symposium, Cambridge, E.T.Brown and J.A.Hudson eds., pp. 231-238.
- Juneja A, Hegde A, Lee FH, Yeo CH (2010). Centrifuge modelling of tunnel face reinforcement using forepoling. *Tunneling Undergr. Space Technol.*, 25(4): 377-381.
- Kim SH, Jeong GH, Kim JS (2006). Predicted and measured tunnel face behaviour during shield tunneling in soft ground. *Tunneling Undergr. Space Technol.*, 21(3-4): 1-264.
- Mitri HS, Edrissi R, Henning J (1994). Finite Element modeling of cable-bolted slopes in hard rock underground mines. *SME Annual Meeting 14–17 February*, New Mexico SME, Albuquerque, pp. 94-116.
- Palmstrom A (2005). Measurements of and correlations between block size and rock quality designation (RQD). *Tunneling Undergr. Space Technol.*, 20(4): 362-377.
- Panthi KK, Nilsen B (2006). Uncertainty analysis of tunnel squeezing for two tunnel cases from Nepal Himalaya. *Int. J. Rock Mech. Min. Sci.*, 44(1): 67-76.
- Read SAL, Richards LR, Perrin ND (1999). Applicability of the Hoek–Brown failure criterion to New Zealand greywacke rocks. *Proceeding 9th International Society for Rock Mechanics Rocscience, 1998. Phase 2 User's Guide*. Rocscience Inc., Toronto, Ontario, Canada.
- Serafim JL, Pereira JP (1983). Considerations of the geomechanics classification of Bieniawski. *Proceedings International Symposium Engineering Geology and Underground Construction*, Balkema, Rotterdam, 1: 1133-1142.
- Singh B, Jethwa JL, Dube AK, Singh B (1992). Correlation between observed support pressure and rock mass quality. *Tunneling Undergr. Space Technol.*, 7:59-74.
- Singh B, Viladkar MN, Samadhiya NK, Mehrotra VK. (1997). Rock mass strength parameters mobilized in tunnels. *Tunneling Undergr. Space Technol.*, 12:147-154.
- Trueman R (1998). An evaluation of strata support techniques in dual life gateroads. PhD Thesis, University of Wales, Cardiff.
- Read SAL, Richards LR, Perrin ND (1999). Applicability of the Hoek–Brown failure criterion to New Zealand greywacke rocks. *Proceeding 9th Int. Soc. Rock Mech. Congress, Paris, 2: 655-660*.
- Stavropoulou M, Exadaktylos G, Saratsis G (2007). A Combined Three-Dimensional Geological-Geostatistical-Numerical Model of Underground Excavations in Rock. *Rock Mech. Rock Eng.*, 40(3): 213-243.
- Tzamos S, Sofianos A (2007). A correlation of four rock mass classification systems through their fabric indices. *Int. J. Rock Mech. Min. Sci.*, 44(4): 477-495.
- Unal E (1983). Design guidelines and roof control standards for coal mine roofs, PhD Thesis, Pennsylvania State University.